

# **Radar Signatures and Near Storm Environmental Parameters of Severe Thunderstorms across Northern New York and Vermont**

*Brooke Taber\*, Rebecca Duell, John Goff, and Andrea LaRocca  
NOAA/National Weather Service  
South Burlington, Vermont*

## **ABSTRACT**

The motivation of this project was to investigate WSR-88D Doppler radar data and near-storm environments to improve severe thunderstorm detection and verification across northern New York and Vermont. This research focused on assessing instability and shear parameters to identify near-storm environments conducive for severe thunderstorm development, along with establishing severe thunderstorm warning thresholds based on reflectivity ( $Z$ ) and differential reflectivity ( $Z_{dr}$ ) values and heights.

All severe thunderstorm warnings and severe weather reports from the National Weather Service (NWS) Burlington, VT, (BTV) County Warning Area (CWA) from 2017 through 2019 during May, June, July, and August were examined. Rapid Refresh (RAP) proximity soundings were utilized to evaluate near-storm thermodynamic and vertical shear parameters. Storms were subsequently classified based on WSR-88D radar reflectivity characteristics into four distinct types; single cell (SC), multi-cell cluster (MCC), multi-cell linear (MCL), and supercell (SP). Radar interrogation of the 50 and 60 dBZ heights were examined, including vertical cross sections of reflectivity and differential reflectivity. An evaluation of traditional height-based reflectivity thresholds at 0°C, -10°C, and -20°C isotherm levels were investigated to identify critical warning thresholds.

The four distinct convective modes demonstrated a large range of environmental parameters conducive for producing severe weather across the BTV CWA. MCL events had the highest shear and lowest instability parameters, while displaying the lowest ( $Z$ ) and ( $Z_{dr}$ ) columns. Additionally, if a  $Z_{dr}$  column of 3 dB or greater was present above the -10°C isotherm, severe weather was observed 89% of the time and 63% of the time if above the 0°C isotherm.

# 1. Introduction

Our knowledge of favorable kinematic and thermodynamic environments for predicting convective storm mode(s) and associated types of severe weather (e.g., tornadoes, hail of at least 2.54 cm (1”) diameter, and winds of at least 26 m s<sup>-1</sup> (50 knots) across the United States has improved significantly through decades of research. Some examples include explanations of organized bow echoes (Fujita 1978), assessment of quasi-linear convective systems (QLCSs) (Weisman and Trapp 2003) and examination of environmental conditions favorable for tornado producing supercells with large magnitudes of Convective Available Potential Energy (CAPE) and deep vertical shear (Rasmussen and Wilhelmson 1983). Brooks and Craven (2002) and Johns and Doswell (1992) have shown various measures of mean-layer CAPE (MLCAPE), most unstable CAPE (MUCAPE), downdraft CAPE (DCAPE) and vertical wind shear correspond well to storm intensity and the associated severe weather threat. Craven and Brooks (2004), found median values of MLCAPE tend to increase with increasing intensity of deep convection with values for non-severe storms <500 J kg<sup>-1</sup>, while severe events showed median values near 750 J kg<sup>-1</sup> and significant events (i.e., tornado intensities of EF2 or greater, wind gusts ≥ 33.4 m s<sup>-1</sup> (65 knots), or hail ≥ 5 cm (2”) diameter) have median MLCAPE values of >1000 J kg<sup>-1</sup>. DCAPE values tend to increase during the progression from thunder to significant hail/wind, with median values increasing from 600 J kg<sup>-1</sup> to over 900 J kg<sup>-1</sup> (Craven and Brooks 2004). A sounding-based climatology by Rasmussen and Blanchard (1998), showed that for supercell

storms, boundary layer (BL) to 6 km bulk shear interquartile values (25<sup>th</sup> to 75<sup>th</sup>) ranged from 12.1-22.1 m s<sup>-1</sup> (21-41 knots), while ordinary (non-supercell) convection saw interquartile values between 5.7 m s<sup>-1</sup> and 15.7 m s<sup>-1</sup> (10 and 30 knots).

The NWS Warning Decision Training Division (WDTD) has established pre-storm environmental thresholds for identifying potential severe weather threats across the United States. For example, when evaluating the severe wind threat (50 knots or greater) within organized QLCSs, the WDTD (2020) best practices for favorable environmental conditions include the following thresholds:

- Most Unstable CAPE (MUCAPE) > 2000 J kg<sup>-1</sup>,
- DCAPE > 980 J kg<sup>-1</sup>,
- Effective Bulk Wind Difference (EBWD) values > 10 m s<sup>-1</sup> (20 knots).

In addition, the WDTD Radar Applications Course (RAC) (WDTD 2020) best practices recommends the following thresholds for 2.54 cm (1 in) hail:

- MUCAPE > 1600 J kg<sup>-1</sup>,
- EBWD > 1 m s<sup>-1</sup> (29 knots),
- 50 dBZ above the melting layer > 4.8 km (16,000 ft),
- Storm top divergence between 36 and 52 m s<sup>-1</sup> (70 and 101 knots),
- Maximum reflectivity > 60 dBZ.

Favorable radar signatures indicative of severe winds within storms have also been established by WDTD. For example, when evaluating a storm on radar for severe winds, the RAC (WDTD 2020) recommends a Mid-Altitude Radial Convergence (MARC) > 25 m s<sup>-1</sup> (50 knots) between 3 and 5 km AGL, a strong leading reflectivity gradient, a bow echo reflectivity signature, and weak echo

channels associated with the descending rear inflow jet.

In contrast, minimal research has focused on convection over northern New York and Vermont due to the relative infrequency of deep, organized thunderstorms. Lombardo and Colle (2010) examined convective storms that produced at least one severe report in the coastal Northeast and found that the average MUCAPE was  $1200 \text{ J kg}^{-1}$  for cellular and linear events, which accounted for more than 70% of severe events in their study. Furthermore, Hurlbut and Cohen (2014) found most severe event days have less than  $1000 \text{ J kg}^{-1}$  of MLCAPE present in observed Northeast proximity soundings. However, as MLCAPE and DCAPE increase, so does the magnitude of summer severe events (Hurlbut and Cohen 2014). While bulk shear magnitudes between severe events over the Northeast and the central United States are relatively similar, a large variability exists in values for individual events (Lombardo and Colle 2010; Hurlbut and Cohen 2014). This large variability in pre-storm environmental conditions highlights some of the challenges faced by forecasters across the Northeast United States in detecting severe weather potential and associated convective mode. In addition, poor low-level radar coverage from complex terrain and associated beam blockage over portions of the Northeast makes sampling of these storms difficult (Figure 1). These challenges, coupled with the sparse population density over the mountainous terrain of northern New York and most of Vermont (Figure 2) also limits the ability to obtain ground truth of severe weather occurrences.

Many of the wind events across northern New York and Vermont lack significant synoptic-scale forcing, exhibit poor radar reflectivity structure, have limited areal coverage, and typically occur in a marginally favorable convective environment. Based on observations and forecaster experience across the eastern United States, tree damage can sometimes occur with winds less than  $25 \text{ m s}^{-1}$  (<50 knots), further complicating warning decisions. Research associated with damaging wind gusts greater than  $25 \text{ m s}^{-1}$  (>50 knots) has focused on reflectivity signatures such as bow echoes and rear inflow notches (House et al. 1989, Przybylinski 1995), meso-vortex velocity patterns (Trapp and Weisman 2003, Atkins et al 2009) and MARC regions (Schmocker et al. 1996). Research by Frugis (2020) examined collapsing Specific Differential Phase ( $K_{DP}$ ) columns and found for both significant and non-significant severe wind events, the  $K_{DP}$  columns were typically between the surface and the freezing level, with the highest elevated values of at least  $5^\circ \text{ km}^{-1}$  generally around 1.5 km (5,000 ft) to 3.0 km (10,000 ft) (AGL) for convection in the Northeastern United States.

In addition, several past studies have addressed the importance and practical applications of assessing differential reflectivity ( $Z_{dr}$ ) columns within convective storms. Scharfenburg et al. (2005) suggest that the presence of taller  $Z_{dr}$  columns may indicate strong updrafts within the storm core. There is also evidence that increases in vertical extent of  $Z_{dr}$  columns above the  $0^\circ\text{C}$  level have direct correlations with increases in low-level reflectivity within the storm at 10 to 30 minute lag times (Picca et al. 2010).

However, the study only focused on a small sample size of storms in Oklahoma. In a comprehensive study, Kumjian et al. (2014) confirmed these studies' hypotheses and furthered understanding of  $Z_{dr}$  column development by coupling a microphysical model with polarimetric radar. In the study, a strong correlation was shown between the maximum height of the 2-dB  $Z_{dr}$  contour and vertical velocities at that level, implying a direct relationship between  $Z_{dr}$  column height and updraft strength. Therefore, assessment of  $Z_{dr}$  column height may allow the radar operator to gage a storm's strength and severity. Values of  $Z_{dr}$  greater than 3 dB have also been shown to indicate the melting of large quantities of small hail within the updraft as the coating of liquid water on the hailstone surface acts to stabilize particle wobbling (Kumjian 2013). More recent research has shown the intensification of  $Z_{dr}$  columns often precedes the development of strong reflectivity cores aloft, and column height is directly correlated with storm strength (Kuster et al. 2020).

While there is considerable difficulty in predicting severe wind occurrence, the same cannot be said with regard to severe hail. Base radar products and interrogation of various dBZ heights within a storm, especially when compared to the freezing level or the  $-20^{\circ}\text{C}$  isotherm can increase confidence of a severe hail threat within a thunderstorm (Frugis and Wasula 2011). Frugis and Wasula (2011) also found 75% of storms producing severe hail had a 50 dBZ echo top of at least 8.1 km (26,500 ft) AGL, while 97% had reflectivity values reaching 60 dBZ or greater with the average 60 dBZ echo top of 7.1 km (23,200 ft) AGL. A study by Donavon and Jungbluth (2007)

found a linear relationship between hail size and the height of the 50 dBZ echo top, while Lemon (1980) discovered a storm would be severe if a 50 to 57 dBZ echo extended above 8.2 km (26,900 ft).

One of the motivating factors of this study is to build on previous national and regional studies in order to grow our understanding of the specific characteristics of storms in the Northeastern U.S. With this increased understanding, it is our goal that local forecasters will be able to adapt warning thresholds established in the central and southern U.S. to be better representative of the more marginal events and environments that are typical of the northeastern U.S., ultimately improving detection of severe storms. This study examines multiple environmental parameters to help forecasters identify potential storm mode, while exploring reflectivity and differential reflectivity columns with respect to  $0^{\circ}\text{C}$ ,  $-10^{\circ}\text{C}$  and  $-20^{\circ}\text{C}$  isothermal levels for determining potential severe thunderstorms across the NWS BTV CWA.

## 2. Data and Methodology

A database was compiled of severe storms with associated severe weather reports across the WFO BTV CWA from 2017 to 2019 during the months of May, June, July and August using Storm Data from the National Centers for Environmental Information (NCEI). Both warned (hits) and unwarned (misses) storms were included in the database. Storms that were warned but did not have associated severe reports (false alarms) were added to

the database through the Iowa Environmental Mesonet NWS Storm Based Warning Verification (IEM Cow). Null events (storms that were not warned and did not lead to severe weather reports) were not examined in this study.

Archived WSR-88D level II base data from the KCXX radar in Colchester, VT, and the KTYX radar in Montague, NY, were obtained from NCEI. A quality control of severe weather reports and associated radar data was performed by removing reports that did not coincide with any reflectivity, double-counted reports and misclassified severe reports. This resulted in 6 removed events. The quality-controlled dataset used for this study included 239 severe wind reports, 25 severe hail reports and zero tornadoes.

### *2.1 Storm Mode Identification Methodology*

The radar site (KCCX or KTYX) with best sampling of the full volumetric data for individual storms was utilized to determine convective mode of each event. Storms were classified into 4 distinct types: 1) single cell (SC), with a criteria of a maximum reflectivity exceeding 40 dBZ and typically lasting at least 15 minutes; 2) multi-cell cluster (MCC) consisting of maximum reflectivity exceeding 40 dBZ, lasting 30 minutes to several hours in duration, with multiple reflectivity cores possible in a disorganized storm structure; 3) multicellular linear (MCL) featuring maximum reflectivity of at least 40 dBZ, which was organized and connected in a linear fashion such as bowing line segments or a QLCS with no minimal length requirement; 4) supercell (SP) exhibiting maximum reflectivity of at least

40 dBZ, lasting > 60 minutes, and a persistent mesocyclone with a rotational velocity of  $>10 \text{ ms}^{-1}$  ( $>20$  knots) within a 7 km radius and depth extending up  $> \frac{1}{4}$  of the storm, lasting at least 10 minutes or more. A reflectivity column was characterized by a continuous 40 dBZ core or greater rising above the  $0^{\circ}\text{C}$  isotherm, suggesting an enhanced storm updraft. 159 storms (79 MCC, 44 MCL, 28 SC, and 8 SP) were classified, with multiple reports possible for each identified convective mode (Figure 3). Given the small SP sample size of only 8 events, the SP convective mode was only used for the reflectivity portion of the study.

### *2.2 Radar and Sounding Analyses*

Archived level II base data from KCXX or KTYX was loaded into Gibson Ridge 2 Analyst (GR2 Analyst) radar view software to examine the dBZ and  $Z_{\text{dr}}$  column structure in a temporal and spatial perspective for each storm mode. Atmospheric thermodynamic sounding profiles were obtained from the Rapid Refresh Model (RAP) and analyzed through SHARPPy (Blumberg et al. 2019) sounding viewer software. Determination of the  $0^{\circ}\text{C}$ ,  $-10^{\circ}\text{C}$  and  $-20^{\circ}\text{C}$  isotherm level was taken from the available sounding in closest proximity and time to severe weather reports from each event and not contaminated by convection (Table 1).

### *2.3 Environmental data*

The time of convective initiation was determined from either KCXX or KTYX radar data and sounding profiles were obtained for the preceding hour prior to convective initiation. Additionally, sounding

locations were determined by their proximity to the storm(s) in question and a brief quality control was performed to assure this sounding was representative of the storm(s) environment. Convective parameters analyzed included: 100-mb MLCAPE, DCAPE, and Effective Bulk Shear (EBWD). See Thompson et al. (2007) for additional information on favorable EBWD parameters for severe thunderstorms.

#### *2.4 Reflectivity Column Interrogation*

The maximum 50 and 60 dBZ core height was calculated utilizing vertical reflectivity cross sections (Figure 4). It's important to remember the radar beam dimensions expand with increasing distance from the radar site. As a result, the sample volume of radar data bins also increases with range from the radar, creating a subjective interpolation for both vertical reflectivity ( $Z$ ) and  $Z_{dr}$  data. If the  $Z$  or  $Z_{dr}$  height data for a particular storm was at the top of the vertical radar range bin, a subjective interpolation was utilized to obtain the storm height information (Figures 4 and 5). Furthermore, the 50 and 60 dBZ height above the 0°C, -10°C and -20°C isotherms were calculated for each convective mode. Radar data up to three scans prior to the report, or three scans prior to the warning for unverified events (false alarms), were used.

#### *2.5 $Z_{dr}$ Column Interrogation*

A  $Z_{dr}$  column was identified by a continuous and deep  $Z_{dr}$  core rising above the 0°C isotherm with values consistently above 3.0 dB. The 3.0 dB threshold value was chosen as this indicated a concentration of large raindrops and masses of melting small

hail aloft, suggesting the presence of strong convective updrafts.  $Z_{dr}$  column heights above the 0°C, -10°C and -20°C isotherms were also calculated for each event to determine potential storm updraft magnitude and resultant hydrometeor loading (Figure 5). Events containing a  $Z_{dr}$  column which did not rise above the 0°C isotherm were counted as not possessing a full column, as the lower portions of those features were frequently beam blocked by terrain or fell below the lowest 0.5 degree scan height of the radar making full interrogation difficult. These factors also limited analyses of true  $Z_{dr}$  column depth on more distant storms, so quantitative assessment of  $Z_{dr}$  column depth across the dataset as a whole was omitted from the study. The same radar column interrogation techniques and severe weather report quality control methods described for reflectivity were used for the  $Z_{dr}$  analysis.

### **3. Results**

#### *3.1 Environmental Results*

Environmental parameters conducive for severe weather across northern New York and Vermont varied widely throughout the convective season. Combinations of 100-mb MLCAPE and EBWD produced a wide variety of storm modes including single cell (SC), multicellular (MC), multicellular linear (MCL) and supercell (SP). The pre-storm environmental data indicated an average MLCAPE of 1094 J kg<sup>-1</sup>, DCAPE values of 768 J kg<sup>-1</sup>, and EBWD values of 16 m s<sup>-1</sup> (31 kt) for MCC, MCL, and SC events combined. Our results indicated MLCAPE, DCAPE, and bulk shear values were considerably less when compared with significant wind/hail

and tornado events studies by Rasmussen and Blanchard (1998) and Craven and Brooks (2004).

Many days over the three-year period (63 of 81 days) saw only a single storm mode, compared to 18 of 81 days which saw evolving storm modes throughout the day. MLCAPE values were highly varied between  $0 \text{ J kg}^{-1}$  (elevated instability rooted above the mixed layer) and  $2384 \text{ J kg}^{-1}$ . This is not surprising given the varying storm modes observed in the study. The interquartile range showed most MLCAPE values were between  $600\text{-}1500 \text{ J kg}^{-1}$  with very few instances of 100-mb MLCAPE greater than  $2000 \text{ J kg}^{-1}$  (4 of 81 days) (Figure 6). EBWD values were equally as varied with values ranging from  $2.6$  to  $34 \text{ m s}^{-1}$  (5 to 67 kt). The majority of shear values fell between  $11\text{-}20 \text{ m s}^{-1}$  (21 to 39 kt) (Figure 7). Similar trends were observed for surface to 3 km SRH (not shown in a chart) with a wide range in values from  $18\text{-}431 \text{ m}^2 \text{ s}^{-2}$ . Increasing median values were observed based on storm type, with the lowest value of  $57 \text{ m}^2 \text{ s}^{-2}$  for MCC events and the highest,  $205 \text{ m}^2 \text{ s}^{-2}$ , occurring with SP events. While DCAPE values as a whole were similarly varied within the 25th and 75th percentiles ( $188\text{-}1417 \text{ J kg}^{-1}$ ), trends were fairly consistent regardless of storm type, approximately  $600\text{-}900 \text{ J kg}^{-1}$  (Figure 8). 0-3 km lapse rates were relatively homogeneous regardless of storm mode ranging between  $5\text{-}9 \text{ }^\circ\text{C km}^{-1}$ . Mean values averaged from  $7.5\text{-}7.7 \text{ }^\circ\text{C km}^{-1}$  and median values from  $7.6\text{-}7.7 \text{ }^\circ\text{C km}^{-1}$  across all storm modes. PWAT values ranged from 21 to 57 mm (0.83 to 2.24 in) across all storm modes except SC which tended to have moderate PWAT values between 33-42 mm (1.3 to 1.65 in).

Several severe weather events occurred on days with weak instability ( $< 200 \text{ J kg}^{-1}$  of 100-mb MLCAPE) and weak to moderate EBWD values of  $2.5\text{-}26 \text{ m s}^{-1}$  (5 to 50 kt). Days with 100-mb MLCAPE less than  $500 \text{ J kg}^{-1}$  were analyzed further to discern if there were any identifiable characteristics of these days compared to those days in which environmental conditions favored severe weather development. 15 of 81 days had MLCAPE values less than  $500 \text{ J kg}^{-1}$  with 13 of 15 days having DCAPE values approximately equal to or greater than MLCAPE (Figure 9). The greater than 1:1 ratio of DCAPE to 100-mb MLCAPE often seen in these marginal thunderstorm environments appears to be a critical ingredient in severe wind production, and is consistent with Vaughn et al. (2017).

### *3.2 Reflectivity Results*

The WFO BTV forecast area typically experiences lower  $Z$  and  $Z_{dr}$  values for severe weather compared to other parts of the United States, especially for MCL events which had the lowest 50 and 60 dBZ heights relative to the other storm types analyzed in this study. No 60 dBZ core above the  $-20^\circ\text{C}$  isotherm was observed among the MCL events examined. The SP and hail events observed the greatest vertical reflectivity extent for both 50 and 60 dBZ cores above the  $0^\circ\text{C}$  and  $-20^\circ\text{C}$  isotherms (Figures 10 and 11). The mean 50 dBZ height above the  $0^\circ\text{C}$  for SP storms was 5.6 km (18,500 ft), and 5.5 km (18,000 ft) for hail events. The mean for MCL storms was 3.5 km (11,600 ft) and wind events was 3.8 km (12,500 ft). The average 60 dBZ height above the  $0^\circ\text{C}$  and  $-20^\circ\text{C}$  for wind and hail events, along with storm mode, showed a similar vertical reflectivity

structure with SP and hail events having the highest 60 dBZ above the 0°C and -20°C, while MCL and wind events were the lowest (Figures 10 and 11). This result indicates events that had less vertical reflectivity structure, were likely driven more by dynamics and wind shear and less on instability.

For the 25 hail events, a 50 dBZ core was present 100% of the time above the 0°C isotherm and 96% of the time above both the -10°C and -20°C levels. Meanwhile, 60 dBZ cores were found 80% of the time above the 0°C line, but only 52% and 32% above the -10°C and -20°C isotherms, respectively. The mean 50 and 60 dBZ height was 8.6 km (28,200 ft) and 5.7 km (18,700 ft) respectively. A box and whisker plot of the 50 and 60 dBZ height for the 25 hail events shows the 25<sup>th</sup> and 75<sup>th</sup> percentile for 50 dBZ were between 8.3 km (27,200 ft) and 9.6 km (31,400 ft); while the 60 dBZ was 4.3 km (14,000 ft) and 7.3 km (24,300 ft) respectively (Figure 12).

The reflectivity structure for our 239 wind events showed lower dBZ thresholds compared to hail events; 90% of wind events had 50 dBZ above the 0°C isotherm, but only 56% saw 50 dBZ values above the -20°C level. Furthermore, 52% of wind events had 60 dBZ above the 0°C isotherm, while only 7% had 60 dBZ above the -20°C isotherm. The mean 50 and 60 dBZ height for wind events was 7.4 km (24,200 ft) and 5.5 km (18,000 ft) respectively. A box and whisker plot for the 239 severe wind events indicated the 25<sup>th</sup> and 75<sup>th</sup> percentile for the 50 and 60 dBZ heights ranged between 6.2 km (20,200 ft) and 8.7 km (28,500 ft) and between 4.5 km (14,600 ft) and 6.4 km (21,100 ft),

respectively (Figure 13). This data suggested hail events have a taller reflectivity structure compared to wind events across our forecast area.

Reflectivity structure was also analyzed based on the storm classification (MCC, MCL, SC, and SP). Combining all events together, 98% had at least 50 dBZ present with 96% having 50 dBZ echo top > 0°C isotherm and 65% > -20°C isotherm. Meanwhile, 69% had 60 dBZ present, with only 62% of events having 60 dBZ > 0°C and 11% above the -20°C level.

Reflectivity thresholds for MCC events indicated 97% had a 50 dBZ core present with a mean height of 7.6 km (24,800 ft), while 72% contained a 60 dBZ core with a mean height of 5.3 km (17,400 ft) (Figure 14). Furthermore, 95% of our MCC events saw 50 dBZ > 0°C level and 66% observed 50 dBZ > -20°C, while only 65% and 11% had 60 dBZ > 0°C and the -20°C isotherm, respectively.

The reflectivity results showed all MCL events had at least 50 dBZ present with a mean height of 6.7 km (21,900 ft), while 60 dBZ was observed only 52% of the time with a mean height of 5.3 km (17,300 ft) (Figure 15). 98% of the MCL events had 50 dBZ > 0°C level, but only 50% of the MCL events indicated 50 dBZ above the -20°C. The 60 dBZ threshold showed only 45% above the 0°C and no MCL events had 60 dBZ > -20°C isotherm. For both MCL and MCC we found our values were slightly lower for severe events when compared to similar studies (Houze et al. 1989, Przybylinski 1995, and Atkins et al. 2009) across the central United States.



We found 96% of SC events had 50 dBZ present with a mean height of 8.1 km (26,900 ft), while 60 dBZ was present 79% of the time with a mean height of 5.8 km (19,100 ft) (Figure 16). 50 dBZ > 0°C and -20°C was observed 96% and 79% of the time respectively, while 75% and 14% had 60 dBZ > 0°C and -20°C isotherms respectively. These results were very similar to studies of SC pulse events across the Northeastern United States (Cerniglia and Snyder 2002; and Frugis and Wasula 2011).

While the sample size was the smallest, SP events exhibited the highest vertical reflectivity structures of all storm modes analyzed. 50 dBZ was present 100% of the time with a mean value of 9.1 km (30,000 ft), while 60 dBZ was observed 88% of the time with a mean dBZ height of 7.3 km (24,000 ft) (Figure 17). A similar trend in the 50 dBZ height above the 0°C and -20°C isotherms was detected, with 100% and 88% respectively. In addition, the results indicated 60 dBZ > the 0°C level was observed 88% of the time, and 63% of the time above the -20°C level.

### 3.3 $Z_{dr}$ Results

Interrogation of  $Z_{dr}$  data showed that 62.9% of all severe events contained a 3 dB column above the 0°C isotherm (Figure 18). If a  $Z_{dr}$  column of 3 dB or greater was present above the -10°C isotherm, severe weather was observed 89% of the time. This suggests at least some utility of this radar product in assessing severe weather potential, especially in combination with other base reflectivity interrogation techniques. Of the three storm types examined (SC, MCC and MCL), the SC type had the highest percentage of tall and

deep  $Z_{dr}$  columns that were above 0°C (75% frequency). This was likely due to a single, strong updraft within the storm core. Single cell, or pulse-type storms, typically form in an environment of higher boundary layer instability and weak surface-6 km shear. While most single cell storms do not reach severe limits, those that do often possess updrafts that are more robust and vertically upright. This increases the likelihood of significant precipitation loading aloft and a higher abundance of large, flat drops or wet hail.

MCL events had the lowest percentage of  $Z_{dr}$  columns of 3 dB or greater at only 56% above the 0°C level and no events above the -20°C isotherm. This is likely due to the highly sheared environments associated with these systems, which inhibit deep, vertically upright updrafts consistently above the 0°C level.  $Z_{dr}$  column height by storm type indicated SC events had the highest columns, while MCL events the lowest columns (Figure 18).

### 3.4 Additional Results

A convective mode vs. time analysis indicated 77% of convection occurred between 1500 Local Standard Time (LST) and 2059 LST and 75% of the MCC and SC events occurred between 1500 and 1959 LST (Figure 19). MCC and SC events had the earliest average event times of 1649 LST and 1707 LST respectively, when surface heating is the strongest and instability the greatest. Meanwhile, MCL events had the latest average event time of 1815 LST and the peak frequency of MCL events (Figure 19) occurring between 1900 and 2059 LST, suggesting these events were high shear/low

instability environments and less reliant on peak daytime heating. The pre-storm environment for MCL events indicated weaker instability values which resulted in less vertical extent in the reflectivity structure for this convective storm mode.

#### 4. Conclusions and Future Work

Preliminary findings from this study will help WFO BTV forecasters better identify pre-storm environmental conditions favorable for severe weather and associated severe radar signatures. Here are some key results:

- DCAPE interquartile range of approximately 600 and 900 J kg<sup>-1</sup>
- Frequent observation of DCAPE to 100-mb MLCAPE ratios of greater than 1:1 suggests this is a critical ingredient in severe wind production
- MLCAPE interquartile range 600 and 1500 J kg<sup>-1</sup>, very few > 2000 J kg<sup>-1</sup>
- EBWD values for majority of our events fell between 11-20 m s<sup>-1</sup> (21 to 39 kt)
- 90% of wind events had 50 dBZ > 0°C, with mean echo top of 7.3 km (24,200 ft)
- 96% of severe hail events had 50 dBZ > -20°C and 80% saw 60 dBZ above the 0°C, with mean value of 8.6 km (28,200 ft) and 5.7 (18,600 ft) respectively
- MCL events mean value of 50 dBZ echo top ≥ 7.2 km (23,600 ft) is present and preferably above the 0°C isotherm level
- MCC events mean value of 50 dBZ echo top to 7.6 km (24,800 ft) and 60 dBZ to 5.3 km (17,400 ft)
- A well-defined Z<sub>dr</sub> column of 3.0 dB rising above the 0°C isotherm is

recommended for identification of severe in SC modes (75% occurrence)

- A well-defined Z<sub>dr</sub> column of 3.0 dB rising above the -10°C isotherm serves as a good proxy for all severe modes (89% occurrence)

This study confirmed weather parameters used in the detection of severe weather are typically of lower magnitude across northern New York and Vermont compared to the Central Plains. A majority of severe events in the WFO BTV CWA were associated with DCAPE values between 600 and 900 J kg<sup>-1</sup>, while MLCAPE was between 600 and 1500 J kg<sup>-1</sup> with very few cases (4 of 81) > 2000 J kg<sup>-1</sup>. EBWD values varied significantly from 2.6 to 34 m s<sup>-1</sup> (5 to 66 kt), but a majority of EBWD values fell between 11-20 m s<sup>-1</sup> (21 to 39 kt).

The WFO BTV forecast area typically experiences lower Z and Z<sub>dr</sub> values for severe weather compared to other parts of the United States, especially for MCL and wind events. Based on 239 wind events studied, we recommend utilizing the mean 50 dBZ echo top height of 7.3 km (24,000 ft) and found 90% (216 out of 239) had 50 dBZ > 0°C for severe warning success. For successful MCL (44 events) severe weather warning operations in WFO BTV CWA, based on the mean value, we recommend 50 dBZ echo top above 7.2 km (23,600 ft) is present and preferably above the 0°C isotherm level. Furthermore, WFO BTV experienced MCC events the most frequently of all convective modes (79) during our 3-year study. Based on the mean value of 50 dBZ echo top to 7.6 km (24,800 ft) and 60 dBZ to 5.3 km (17,400 ft) for all events; those are our recommended thresholds for

successful identification of severe thunderstorm winds.

Severe hail events (25 events) typically had higher 50 and 60 dBZ vertical reflectivity structure. For severe hail best practices, we identified a 50 dBZ core above  $-20^{\circ}\text{C}$  (96% of cases) and 60 dBZ core above  $0^{\circ}\text{C}$  (80% of cases). Since hail is strongly dependent on the thermodynamic environment, we recommend viewing reflectivity relative to the  $0^{\circ}\text{C}$  and  $-20^{\circ}\text{C}$  (rather than height AGL) for achieving better highest verification results.

Final recommendations are that  $Z_{\text{dr}}$  column interrogation shows some value in assessing severe storm potential during all convective regimes when used in combination with other techniques. Within the broad spectrum of all storm types, its utility in single cell, pulse events (type SC) shows the highest potential as a severe weather indicator. In these cases, a well-defined column of 3.0 dB rising above the  $0^{\circ}\text{C}$  isotherm is a recommended warning threshold.

While examining  $Z$  and  $Z_{\text{dr}}$  height thresholds, it is imperative severe weather warning forecasters utilize this data in conjunction with other radar data interrogation techniques to make the best warning decision possible. In addition, when interrogating a storm for severe wind or hail, it is critical that the warning forecaster maintains situational awareness and adjusts warning thresholds and decisions based on real-time and credible severe weather observations. A complete analysis of the pre-storm environment is crucial for successful severe weather warning operations, along

with anticipating how conditions could change during an event and potential impacts on warning thresholds.

Future work could include examining additional events, including null cases to better confirm and quantify our pre-storm environment, reflectivity and  $Z_{\text{dr}}$  results. Furthermore, Multi-Radar/Multi-Sensor (MRMS) data could be examined to determine how well the hail products perform and develop additional critical thresholds for improved warning decisions. WFO Burlington plans to update local severe weather radar procedures and warning reference materials to highlight our findings, which is expected to help warning forecasters with the detection of severe weather signatures across our CWA.

## Acknowledgements

Radar imagery was generated using GR2Analyst, Gibson Ridge Software Company [http://www.grlevelx.com/gr2analyst\\_2/](http://www.grlevelx.com/gr2analyst_2/)

Disclaimer. Reference to any specific commercial products, process, or service by trade name, trademark, manufacturer, or otherwise, does not constitute or imply its recommendation, or favoring by the United States Government or NOAA/National Weather Service. Information from this publication shall not be used for advertising or product endorsement purposes.

The authors would like to thank Peter Banacos, Burlington WFO SOO and Jeff Waldstreicher and Jordan Rabinowitz from NWS Eastern Region Scientific Services Division (SSD) for their thorough and timely review of this publication.

## References

- Atkins, N.T. and M. St. Laurent, 2009: Bow echo mesovortices. Part I: Processes that influence their damage potential. *Mon. Wea. Rev.*, **137**, 1497-1513.  
<https://journals.ametsoc.org/view/journals/mwre/137/5/2008mwr2649.1.xml>
- Blumberg, W.G, Halbert, K.T., Supinie, T.A., Marsh, P.T., Thompson, R., and J. Hart, 2019: SHARPPy Documentation. Accessed 26 April 2021,  
<https://sharppy.github.io/SHARPPy/index.html>.
- Brooks, H. E., and J. P. Craven, 2002: A database of proximity soundings for significant severe thunderstorms, 1957–2003. Preprints, *21st Conf. on Severe Local Storms*, San Antonio, TX, Amer. Meteor. Soc., 16.2.  
[https://ams.confex.com/ams/SLS\\_WAF\\_NWP/techprogram/paper\\_46680.htm](https://ams.confex.com/ams/SLS_WAF_NWP/techprogram/paper_46680.htm)
- Cerniglia, C.S. and W.R. Snyder, 2002: Development of warning criteria for severe pulse thunderstorms in the northeastern United States using the WSR-88D. *Eastern Region Technical Attachment, No 2002-03*, National Weather Service, NOAA, Dept. of Commerce, Bohemia, NY, 14 pp.  
<https://www.weather.gov/media/erh/ta2002-03.pdf>
- Craven, J.P. and H. E. Brooks, 2004: Baseline climatology of sounding derived parameters associated with deep, moist convection. *Natl. Wea. Dig.*, **28**, 13-24.  
<http://nwafiles.nwas.org/digest/papers/2004/Vol28/Pg13-Craven.pdf>
- Donavon, R.A., and K.A. Jungbluth, 2007: Evaluation of a technique for radar identification of large hail across the upper Midwest and central Plains of the United States. *Wea. Forecasting*, **22**, 244-254.  
<https://doi.org/10.1175/WAF1008.1>
- Frugis, B. J., 2020: The Use of Collapsing Specific Differential Phase Columns to Predict Significant Severe Thunderstorm Wind Damage across the Northeastern United States. *Eastern Region Technical Attachment, No 2020-04*, National Weather Service, NOAA, Dept. of Commerce, Bohemia, NY, 16 pp.  
<https://www.weather.gov/media/erh/ta2020-04.pdf>
- Frugis, B. J., T. A. Wasula, 2011: Development of warning thresholds for one inch or greater hail in the Albany New York county warning area. *Eastern Region Technical Attachment, No 2011-05*, National Weather Service, NOAA, Dept. of Commerce, 24 pp., Bohemia, NY.  
<https://www.weather.gov/media/erh/ta2011-05.pdf>
- Fujita, T. T., 1978: Manual of downburst identification for project NIMROD. Satellite and Mesometeorology Research Paper 156, Dept. of Geophysical Sciences, University of Chicago, 104 pp.
- Houze, R. A. Jr., S. A. Rutledge, M.I. Biggerstaff, and B.F. Smull, 1989: Interpretation of Doppler weather radar displays of mid-latitude mesoscale convective systems. *Bull. Amer. Meteor. Soc.*, **70**, 608- 618.  
[https://journals.ametsoc.org/view/journals/bams/70/6/1520-0477\\_1989\\_070\\_0608\\_iodwrd\\_2\\_0\\_co\\_2.xml](https://journals.ametsoc.org/view/journals/bams/70/6/1520-0477_1989_070_0608_iodwrd_2_0_co_2.xml)
- Hurlbut, M. M., and A. E. Cohen, 2014: Environments of northeast U.S. severe thunderstorm events from 1999 to 2009. *Wea. Forecasting*, **29**, 3–22,
- Johns, R. H., and C. A. Doswell III, 1992: Severe local storms forecasting. *Wea. Forecasting*, **7**, 588–612.  
[https://doi.org/10.1175/1520-0434\(1992\)007%3C0588:SLSF%3E2.0.CO;2](https://doi.org/10.1175/1520-0434(1992)007%3C0588:SLSF%3E2.0.CO;2)

Kumjian, M. R., 2013: Principles and Applications of Dual-Polarization Weather Radar. Part I: Description of the Polarimetric Radar Variables. *J. Operational Meteor.*, **1** (19), 226-242. <https://doi.org/10.15191/nwajom.2013.0119>

Kumjian, M. R., and coauthors, 2014: The Anatomy and Physics of Z<sub>DR</sub> Columns: Investigating a polarimetric radar signature with a spectral Bin Microphysical Model. *J. Appl. Meteor. Climatol.*, **53**, 1820–1843. <https://doi.org/10.1175/JAMC-D-13-0354.1>

Kuster, C.M., T.J. Schuur, T.T. Lindley and J.C. Snyder, 2020: Using Z<sub>dr</sub> columns in forecaster conceptual models and warning decision-making. *Wea. Forecasting*, **35**, 2507-2522. <https://doi.org/10.1175/WAF-D-20-0083.1>

Lemon, L. R., 1980: Severe thunderstorm radar identification techniques and warning criteria. *NOAA Tech. Memo. NWS NSSFC-3*, 60 pp. [Available from NOAA Central Library, 1315 East–West Highway, Silver Spring, MD 20910.].

Lombardo, K. A., and B. A. Colle, 2010: The spatial and temporal distribution of organized convective structures over the northeast and their ambient conditions. *Mon. Wea. Rev.*, **138**, 4456–4474, <https://doi.org/10.1175/2010MWR3463.1>.

Picca, J. C., M. R. Kumjian, and A. V. Ryzhkov, 2010: ZDR columns as a predictive tool for hail growth and storm evolution. 25<sup>th</sup> Conf. on Severe Local Storms, Denver, CO, Amer. Meteor. Soc., 11.3, [Available online at [https://ams.confex.com/ams/25SLS/techprogram/paper\\_175750.htm](https://ams.confex.com/ams/25SLS/techprogram/paper_175750.htm)].

Przybylinski, R. W., 1995: The bow echo: Observations, numerical simulations, and severe weather detection methods. *Wea. Forecasting*, **10**, 203-218. [https://journals.ametsoc.org/view/journals/efo/10/2/15200434\\_1995\\_010\\_0203\\_tbeons\\_2\\_0\\_co\\_2.xml](https://journals.ametsoc.org/view/journals/efo/10/2/15200434_1995_010_0203_tbeons_2_0_co_2.xml)

Rasmussen, E. N., and D. O. Blanchard, 1998: A baseline climatology of sounding-derived supercell and tornado forecast parameters. *Wea. Forecasting*, **13**, 1148-1164. [https://doi.org/10.1175/1520-0434\(1998\)013%3C1148:ABCOSD%3E2.0.CO;2](https://doi.org/10.1175/1520-0434(1998)013%3C1148:ABCOSD%3E2.0.CO;2)

\_\_\_\_\_, and R. B. Wilhelmson, 1983: Relationships between storm characteristics and 1200 GMT hodographs, low level shear, and stability. Preprints, 13th Conf. on Severe Local Storms, Tulsa, OK, *Amer. Meteor. Soc.*, J5–J8.

Scharfenburg, K. A., and coauthors, 2005: The Joint Polarization Experiment: Polarimetric radar in forecasting and warning decision making. *Wea. Forecasting*, **20**, 775-788, <https://doi.org/10.1175/WAF881.1>

Schmocker, G. K., R. W. Przybylinski, and Y. J. Lin, 1996: Forecasting the initial onset of damaging downburst winds associated with a Mesoscale Convective System (MCS) using the Mid-Altitude Radial Convergence (MARC) signature. Preprints, 15th Conf. On Weather Analysis and Forecasting, Norfolk VA, Amer. Meteor. Soc., 306-311

Thompson, R.L., C. M. Mead, and R. Edwards, 2007: Effective storm-relative helicity and bulk shear in supercell thunderstorm environments. *Wea. Forecasting*, **22**, 102–115, <http://dx.doi.org/10.1175/WAF969.1>.

Trapp, R. J., and M. L. Weisman, 2003: Low-level mesovortices within squall lines and bow echoes. Part II: Their genesis and implications. *Mon. Wea. Rev.*, **131**, 2804–2823. [https://doi.org/10.1175/1520-0493\(2003\)131<2804:LMWSLA>2.0.CO;2](https://doi.org/10.1175/1520-0493(2003)131<2804:LMWSLA>2.0.CO;2)

Vaughan, M. T., B. H. Tang, and L. F. Bosart, 2017: Climatology and analysis of high-impact, low predictive skill severe weather events in the Northeast United States. *Wea. Forecasting*, **32**, 1903-1919, <https://doi.org/10.1175/WAF-D-17-0044.1>

WDTD, 2020: Warning Methodology. Accessed 26 April 2021, <https://training.weather.gov/wdtd/courses/rac/documentation/rac20-warn-method.pdf>

Weisman, M. L., and Trapp R. J. 2003: Low-level mesovortices within squall lines and bow echoes. Part I: Overview and dependence on environmental shear. *Mon. Wea. Rev.*, **131**, 2779–2803. [https://doi.org/10.1175/1520-0493\(2003\)131%3C2779:LMWSLA%3E2.0.CO;2](https://doi.org/10.1175/1520-0493(2003)131%3C2779:LMWSLA%3E2.0.CO;2)

<b>RAP model site</b>	<b>Location</b>	<b>Frequency in analysis</b>
KBTV	Burlington, VT	50
KGTB	Fort Drum, NY	9
KMPV	Montpelier, VT	15
KMSS	Massena, NY	11
KPBG	Plattsburgh, NY	13
KRUT	Rutland, VT	27
KSLK	Saranac Lake, NY	10
KVSF	Springfield, VT	8
K1V4	St. Johnsbury, VT	8

**Table 1.** RAP model sounding locations and usage frequency in Z and  $Z_{dr}$  analysis.

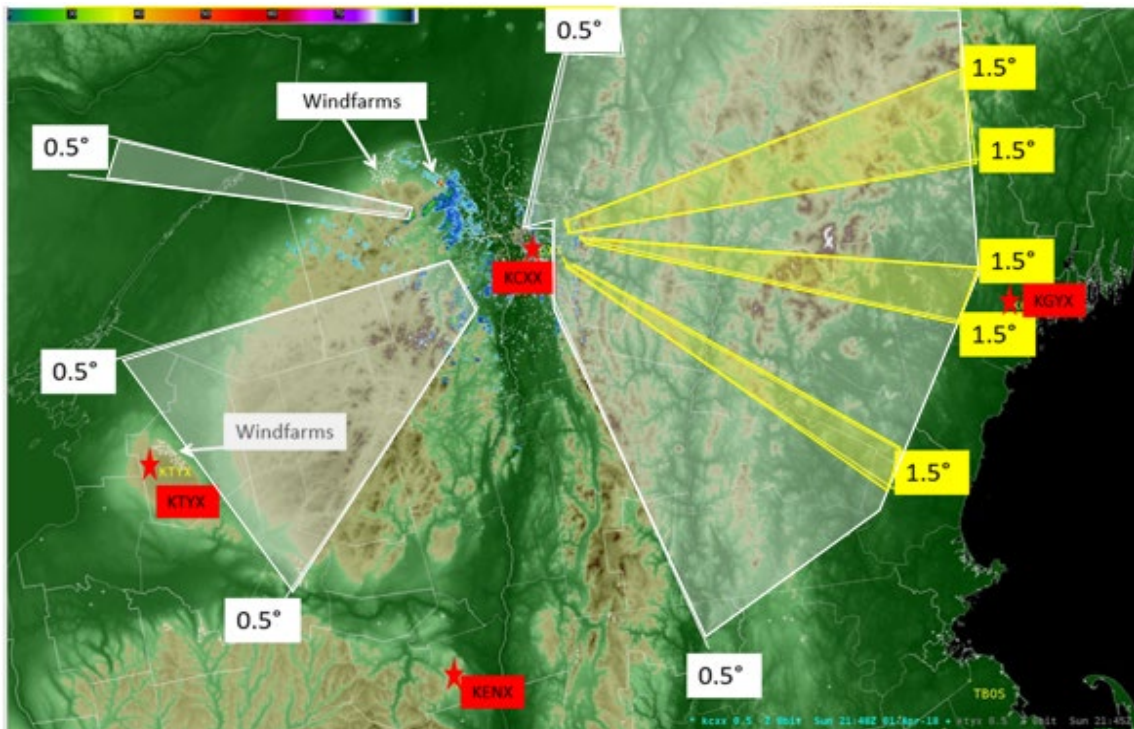


**Figure 1:** WSR-88D radar locations and high resolution topography map with 0.5° (white) and 1.5° (yellow) elevation slices indicating areas of beam blockage by terrain from the KCXX WSR-88D radar in Colchester, VT. Locations of wind farms negatively impacting the quality of radar data are also annotated.

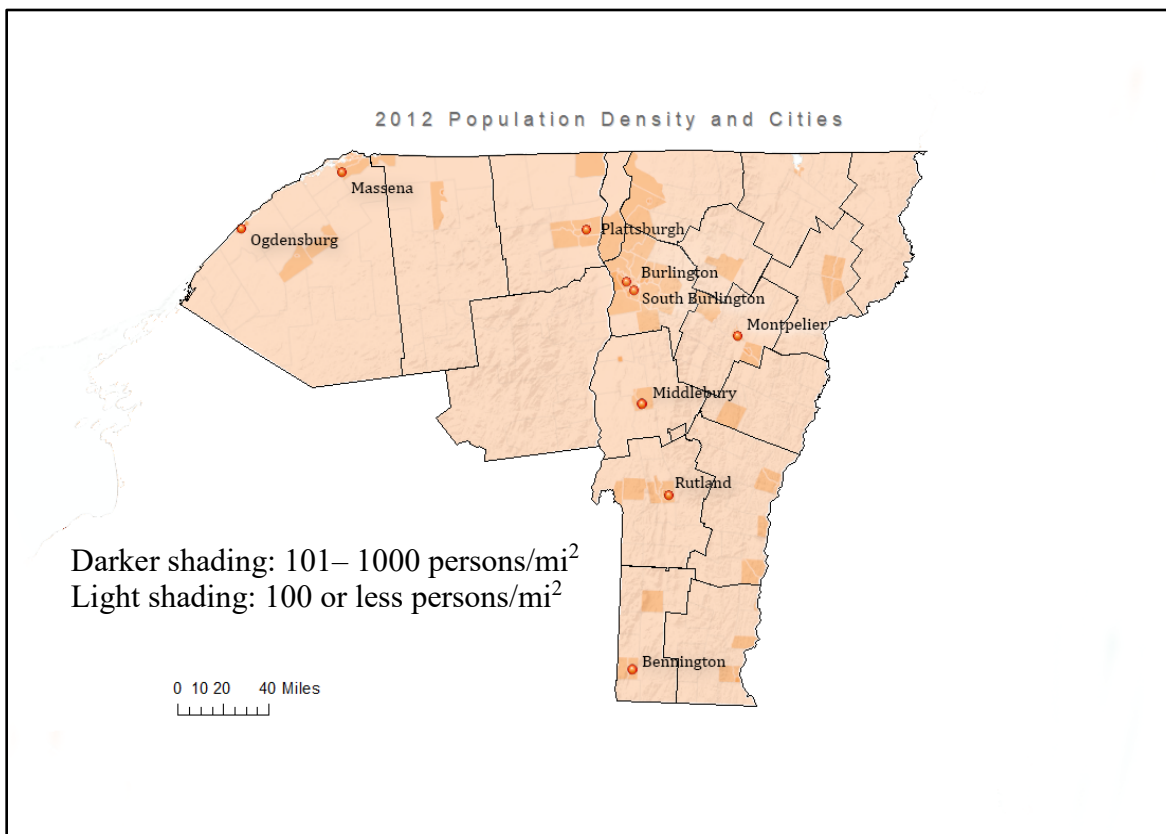


**Figure 2:** 2012 Population density and cities across northern New York and all of Vermont.



# Radar Storm Classification Examples

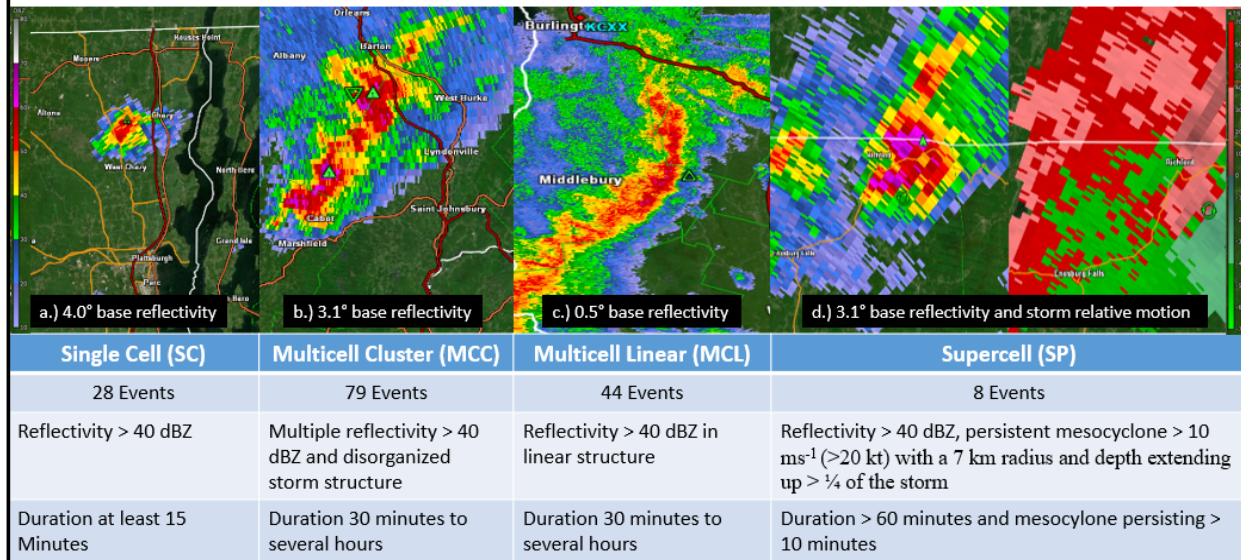


**Figure 3:** Radar storm classification examples, a.) KCXX 4.0° base reflectivity single cell, b.) KCXX 3.1° base reflectivity multi-cell cluster, c.) KCXX 0.5° base reflectivity multi-cell linear and d.) KCXX 3.1° base reflectivity and storm relative motion supercell.

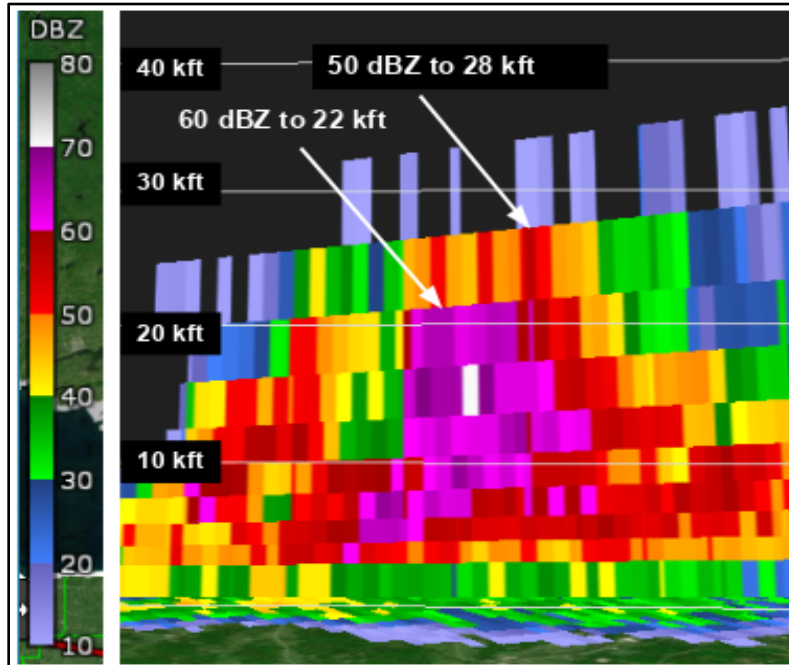


**Figure 4:** Gibson Ridge 2 Analyst (GR2 Analyst) reflectivity “dBZ” cross section near Richford, VT on 4 May 2018, highlighting data collection methodology for dBZ heights.

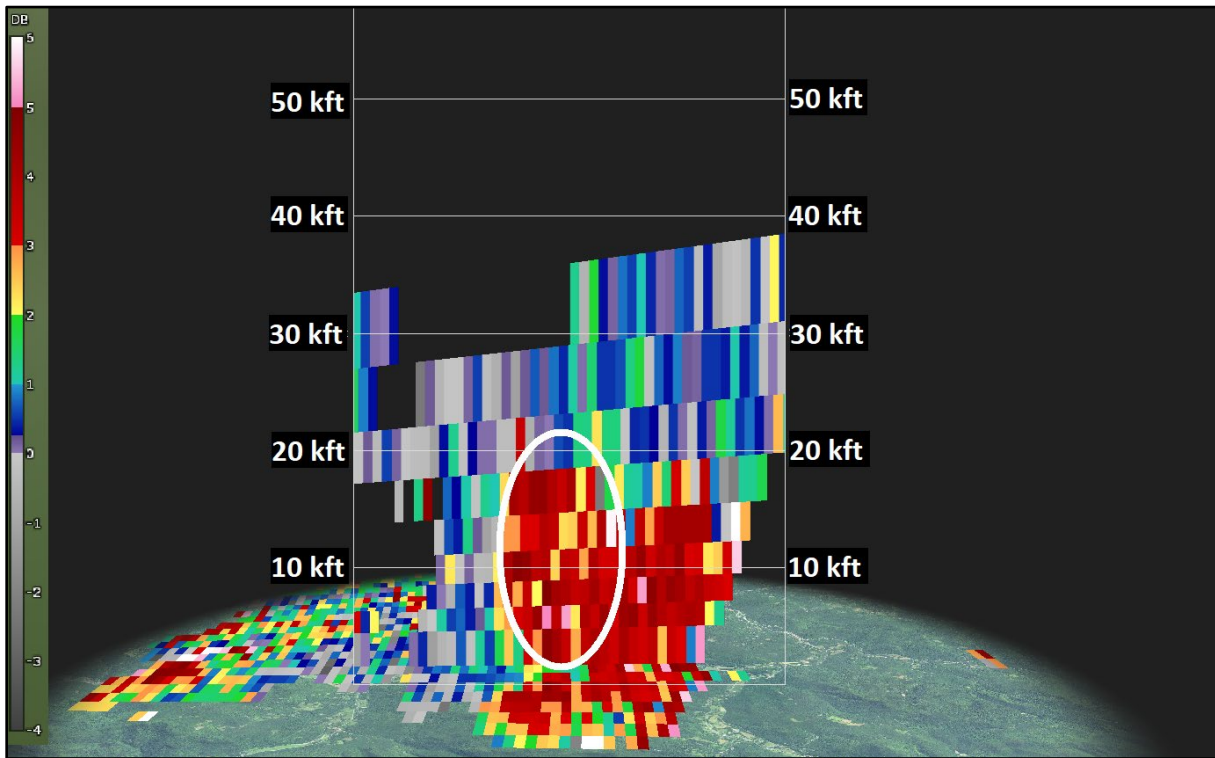


Figure 5: Sample  $Z_{dr}$  column cross-section from a severe storm near Bethel, VT on 20 July 2019 (white oval).

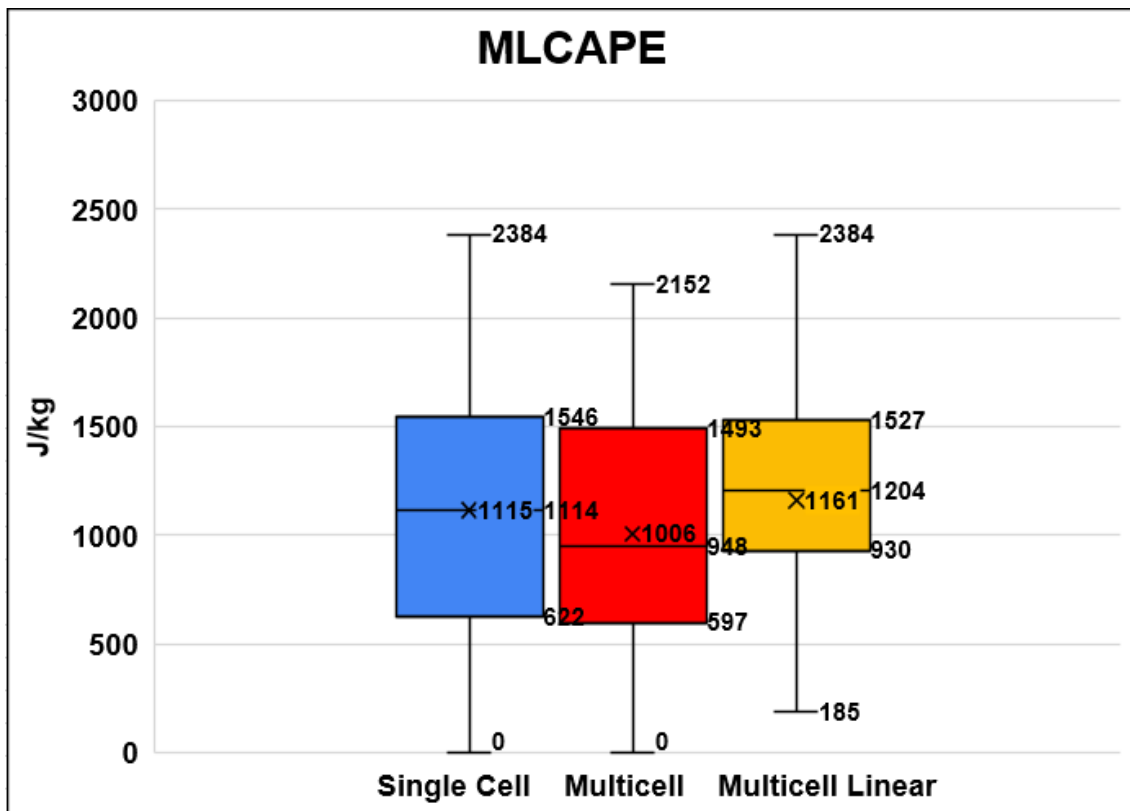


Figure 6: MLCAPE ( $J\ kg^{-1}$ ) by storm classification type. The top and bottom of the shaded boxes denote the 75th and 25th percentile values, respectively, with the horizontal line the median and the “X” the mean. The whiskers extend upward to the 90th and downward to the 10th percentiles.

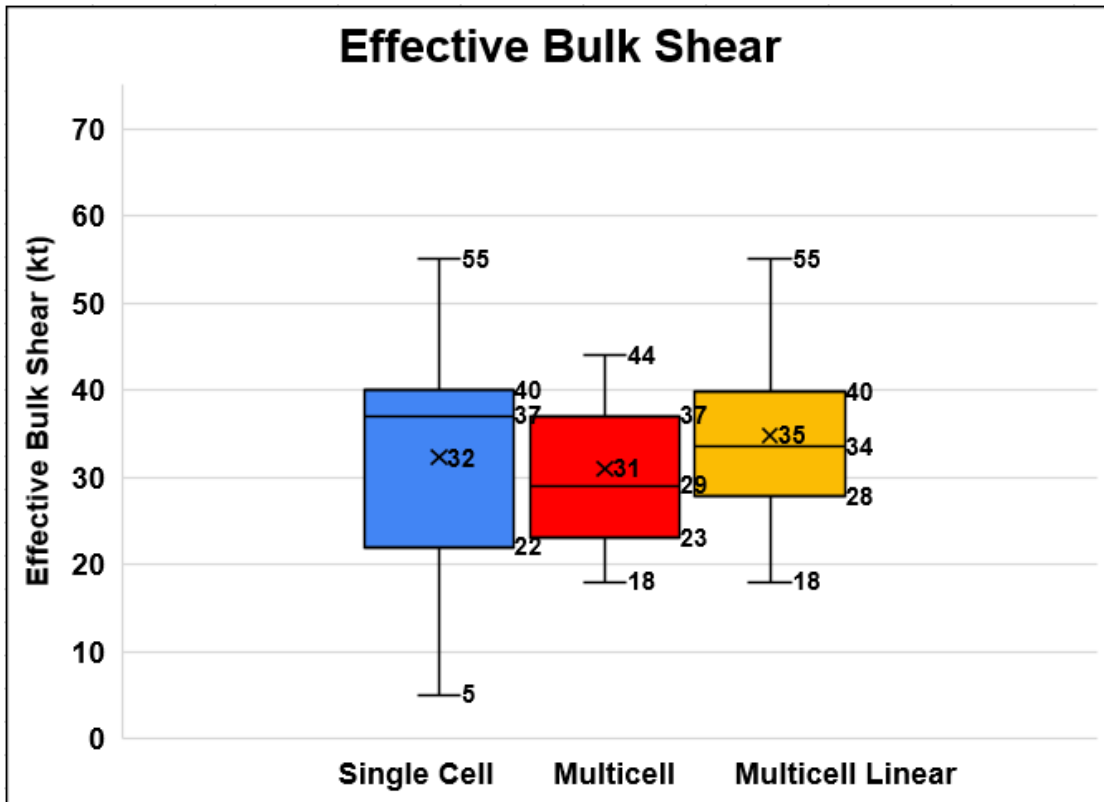


Figure 7: As in Fig. 6, except for Effective Bulk Shear (knots) by storm classification type.

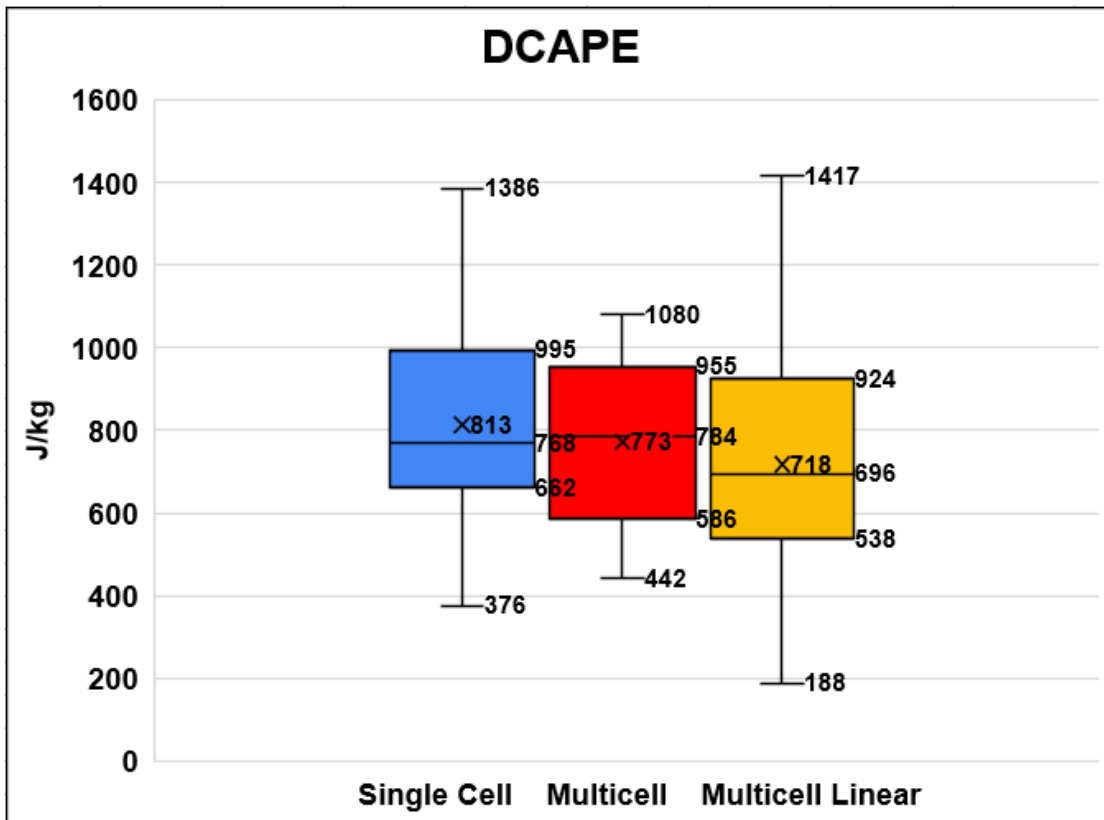


Figure 8: As in Fig. 6, except for DCAPE ( $J\ kg^{-1}$ ) by storm classification type.

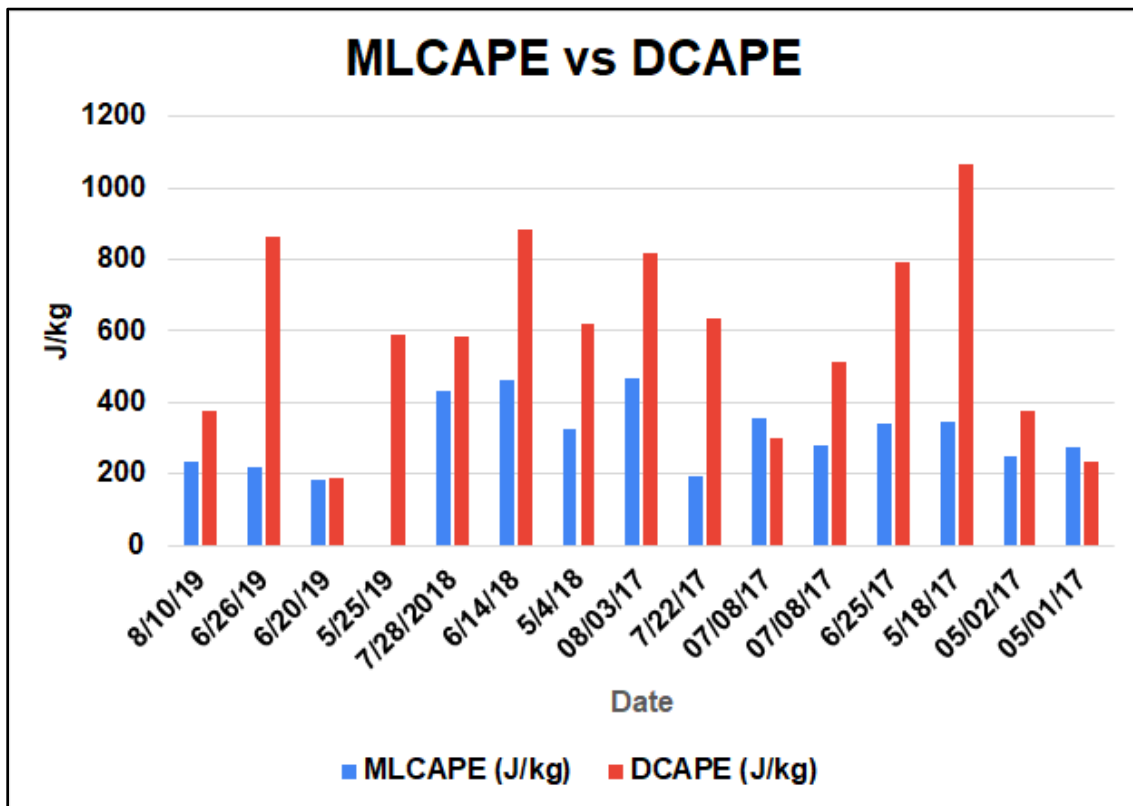


Figure 9: MLCAPE vs. DCAPE ( $J\ kg^{-1}$ ) for events with 100-mb MLCAPE less than  $500\ J\ kg^{-1}$ .

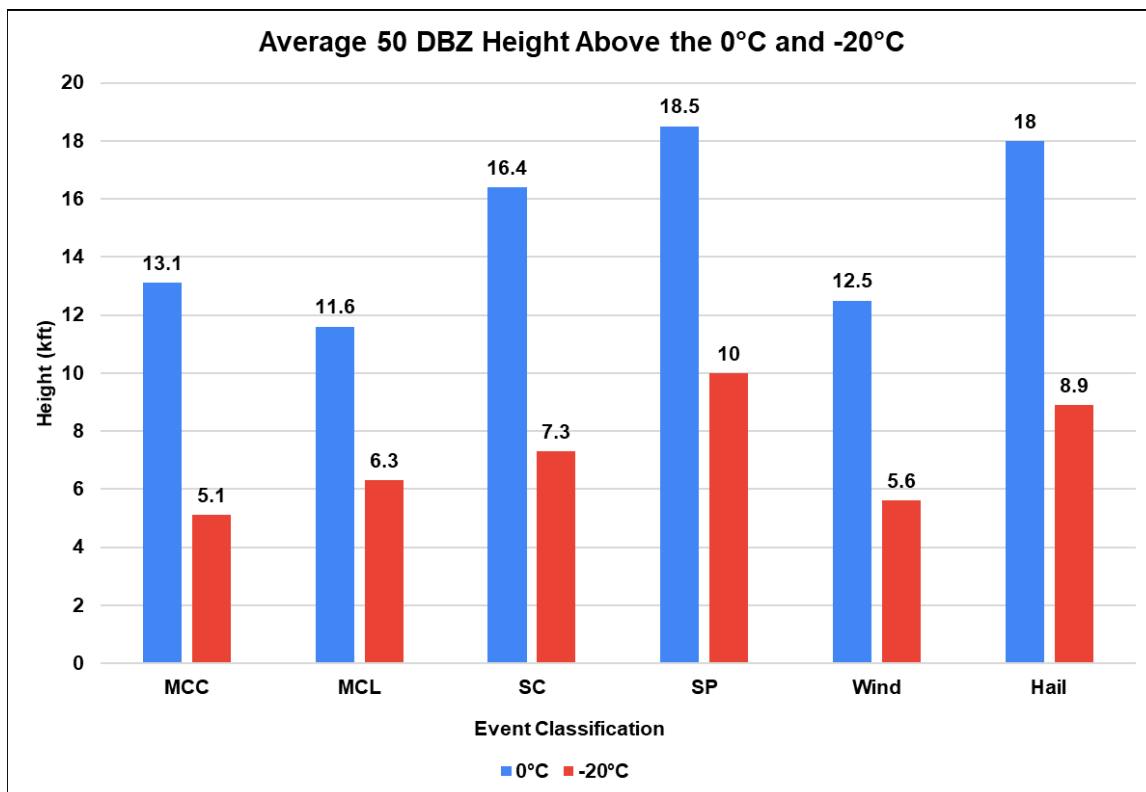


Figure 10: The average 50 dBZ height (in kft) above the  $0^{\circ}C$  and  $-20^{\circ}C$  for multi-cell cluster (MCC), multi-cell linear (MCL), single cell (SC), and supercell (SC) cases, and all wind and hail events.

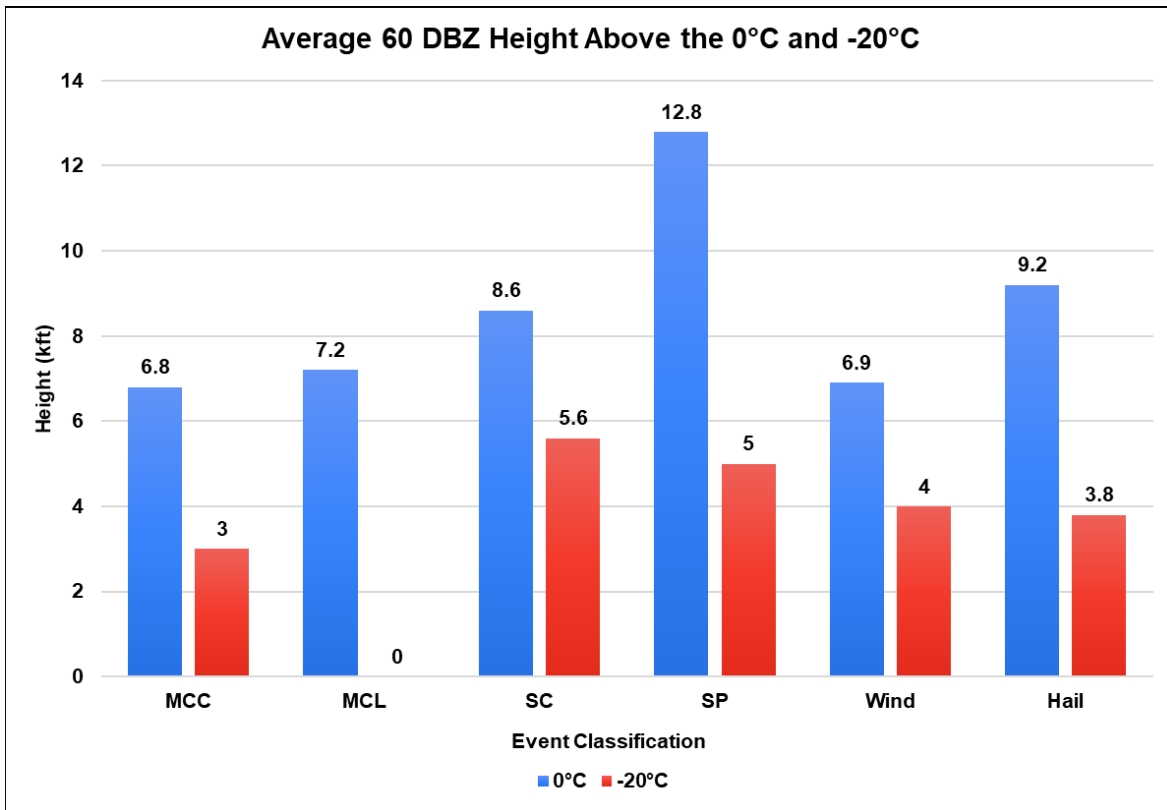


Figure 11: The average 60 dBZ height for 0°C and -20°C for multi-cell cluster (MCC), multi-cell linear (MCL), single cell (SC), and supercell (SC) cases, and all wind and hail events.

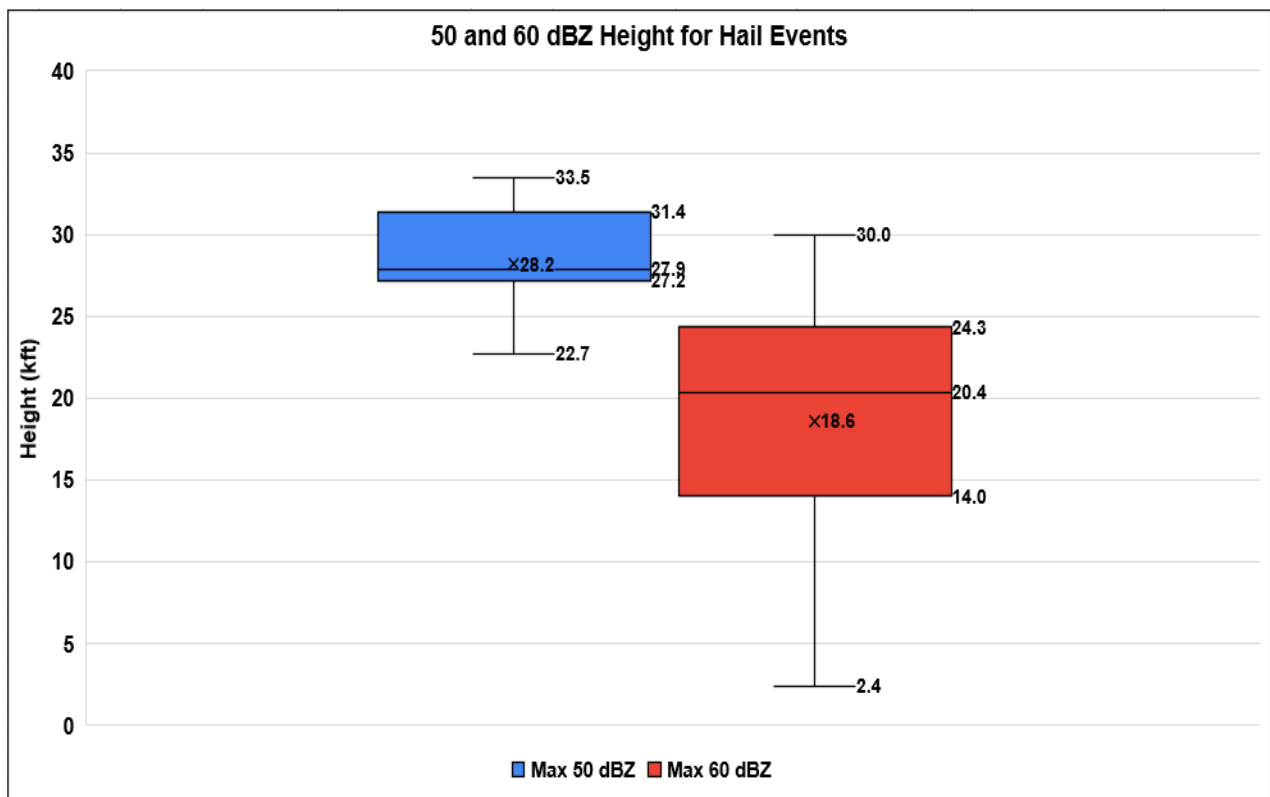


Figure 12: As in Fig. 6, except for the 50 and 60 dBZ height (kft) for hail events.

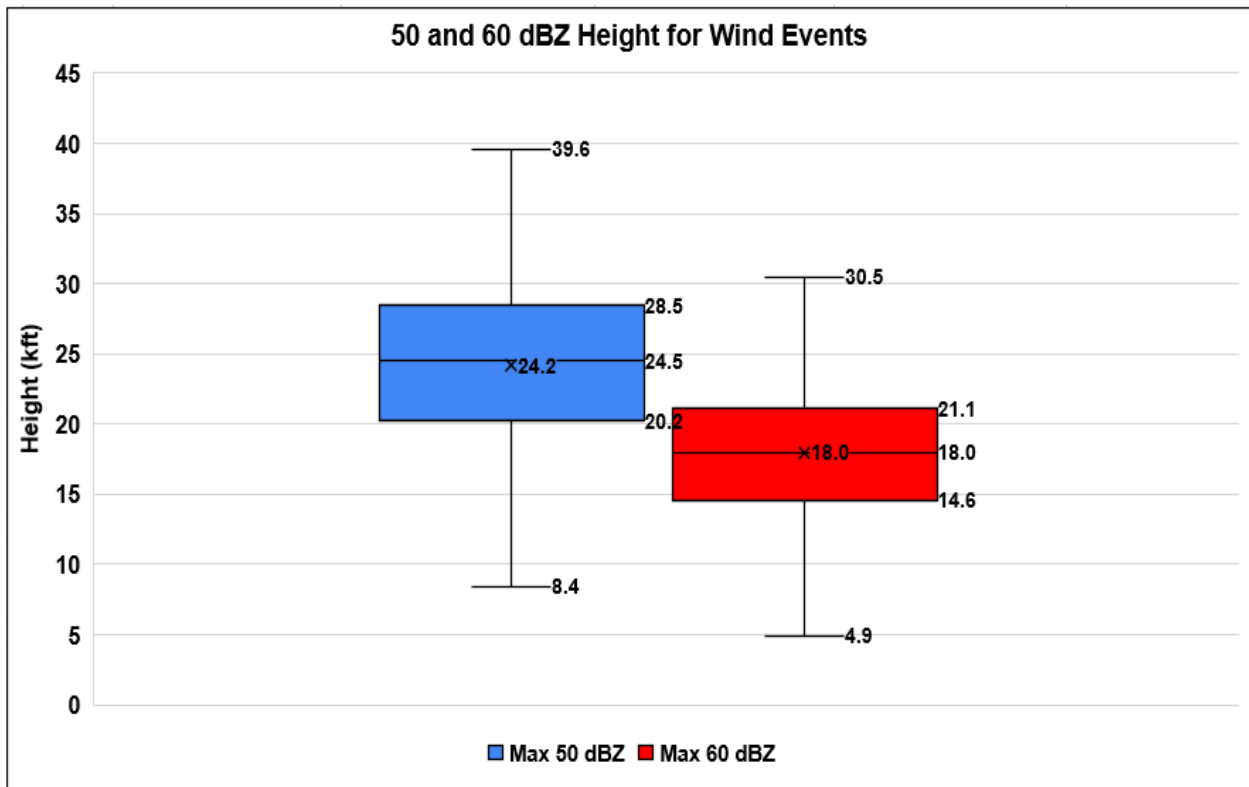


Figure 13: As in Fig. 6, except for the 50 and 60 dBZ height (kft) for wind events.

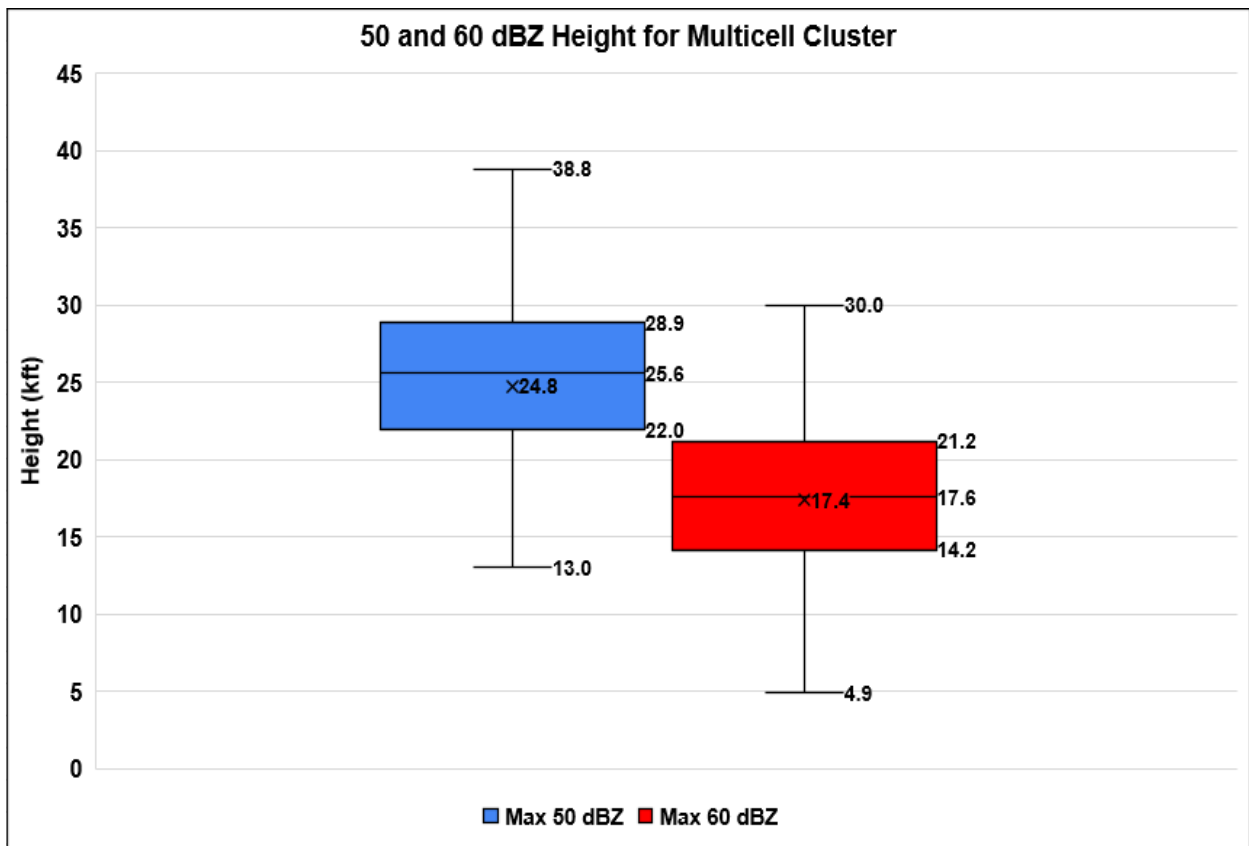


Figure 14: As in Fig. 6, except for the 50 and 60 dBZ height (kft) for multi-cell cluster (MCC).

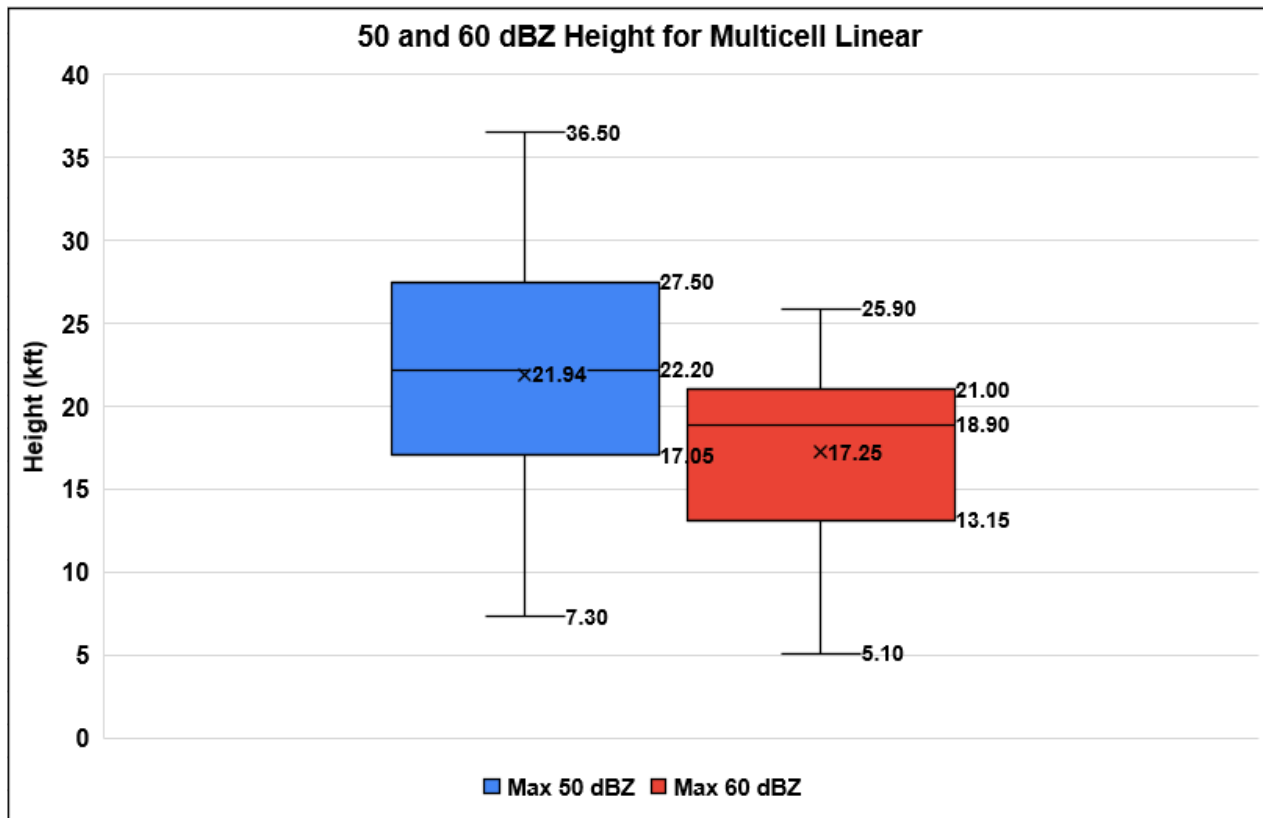


Figure 15: As in Fig. 6, except for the 50 and 60 dBZ height (kft) for multi-cell linear (MCL).

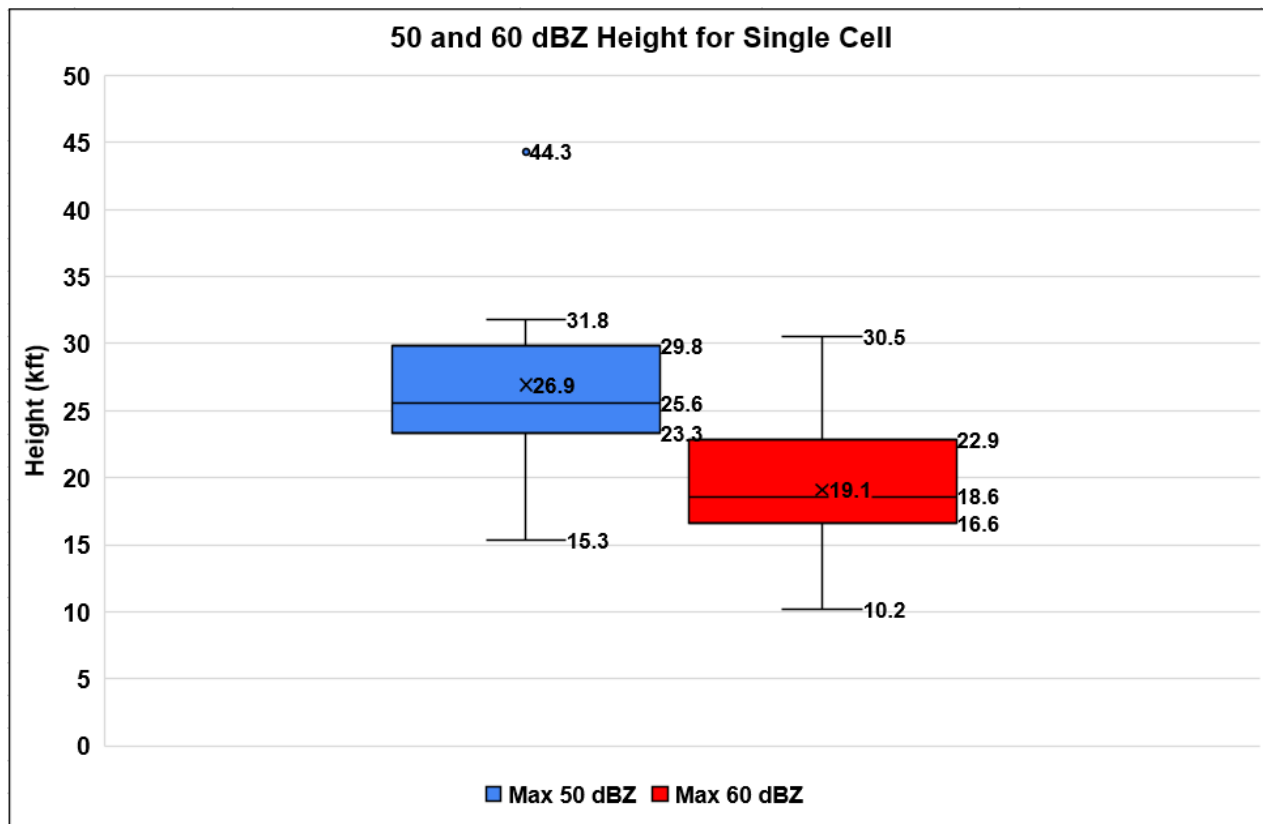


Figure 16: As in Fig. 6, except for the 50 and 60 dBZ height (kft) for single cell (SC).

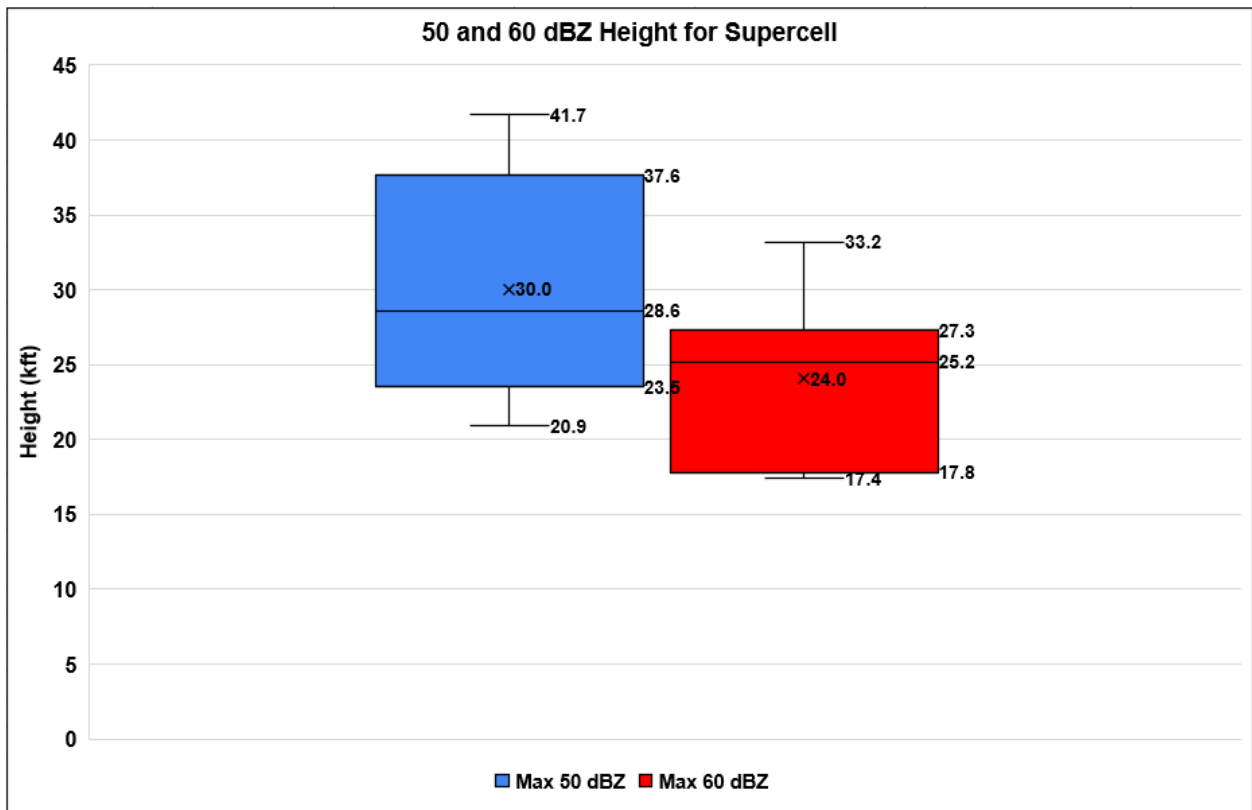


Figure 17: As in Fig. 6, except for the 50 and 60 dBZ height (kft) for supercell (SP).

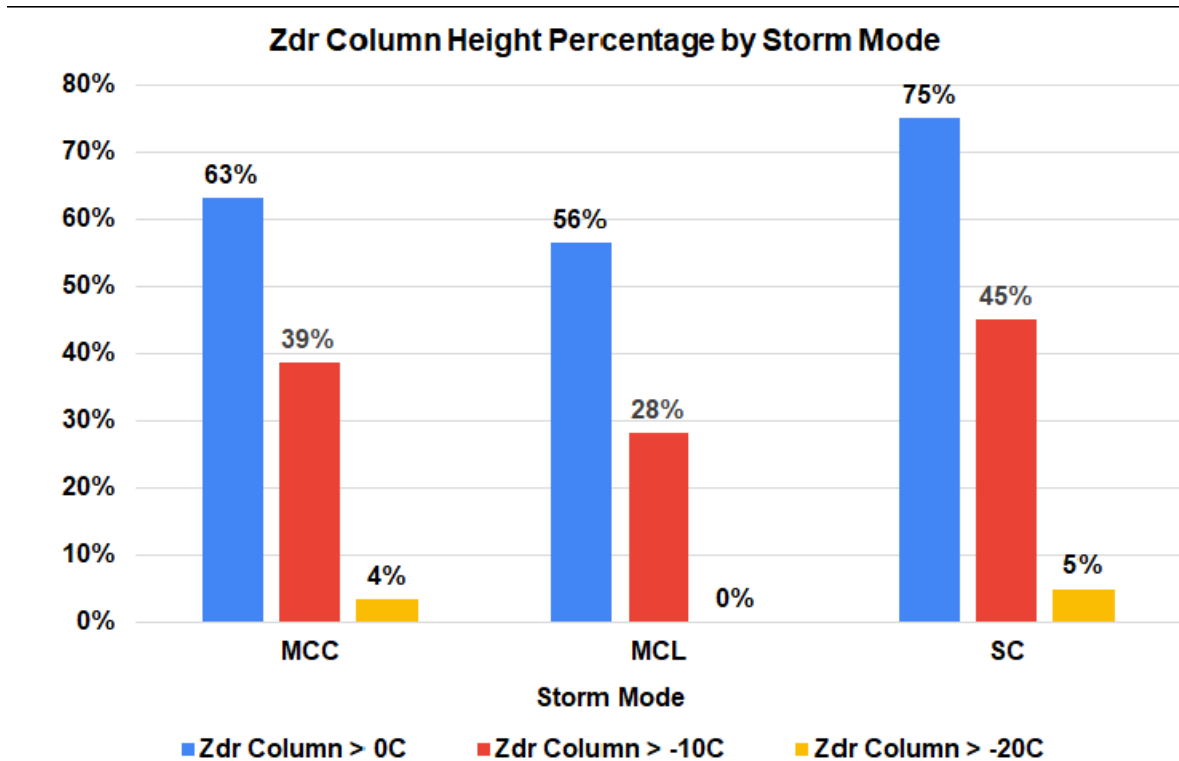
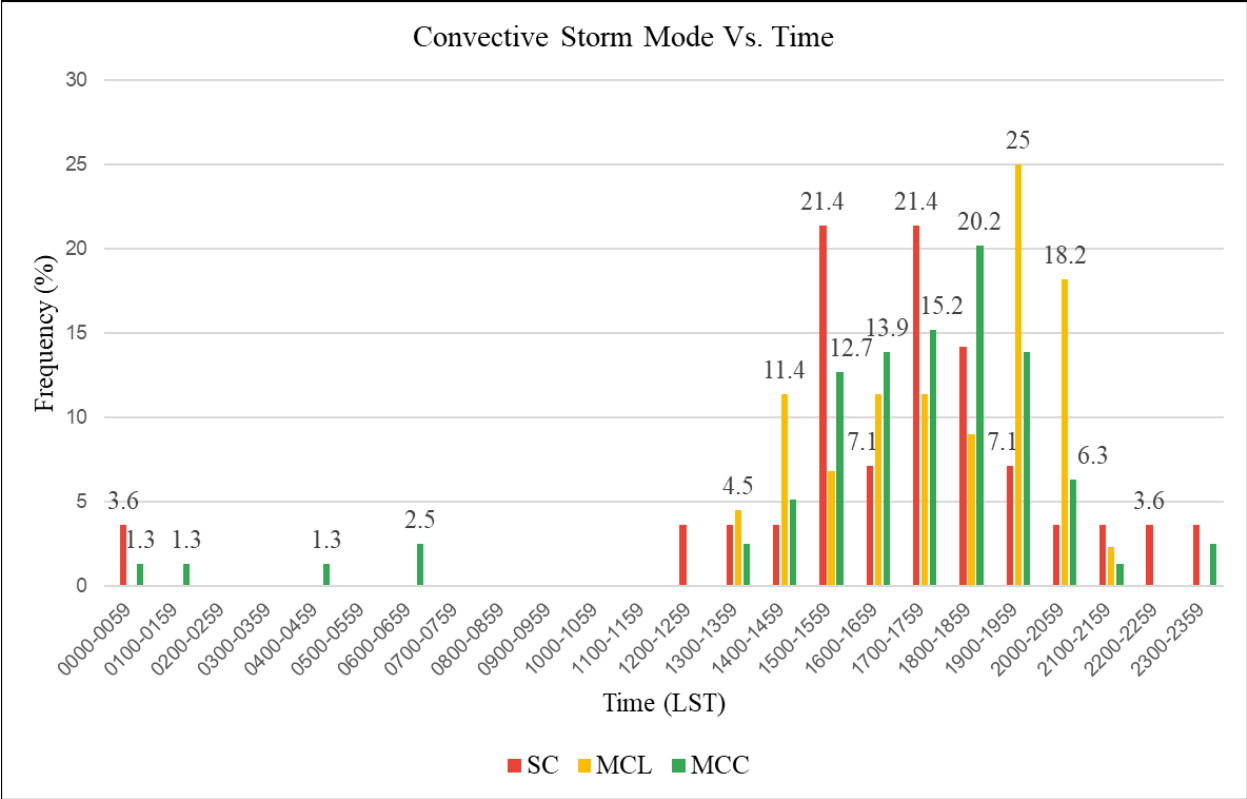


Figure 18:  $Z_{dr}$  column height percentage by storm mode. A  $Z_{dr}$  column was identified by a continuous and deep area of  $Z_{dr}$  with values consistently above 3.0 dB rising above the 0°C isotherm.





**Figure 19.** Convective storm mode single (SC), multi-cell linear (MCL), and multi-cell cluster (MCC) vs. time with frequency as a percentage.